THE JOURNAL OF PHYSICAL CHEMISTRY B
A JOURNAL OF THE AMERICAN CHEMICAL SOCIETY

pubs.acs.org/JPCB

Article

Thermal Degradation Energy Landscapes of Fluorofentanyls: Probing the Mechanisms and Energetics of Bond Breaking

Published as part of The Journal of Physical Chemistry B special issue "At the Cutting Edge of Theoretical and Computational Biophysics".

Bharat Poudel,* Joshua J. Whiting, Juan M. Vanegas, and Susan B. Rempe*

Cite This: *J. Phys. Chem. B* 2026, 130, 3–10

Read Online

ACCESS | Metrics & More | Article Recommendations | Supporting Information

ABSTRACT: To aid in the detection of fluorofentanyls, which degrade with exposure to heat such as during consumption by smoking, it is essential to understand the potential degradation products. However, the degradation products of fluorofentanyls are not well characterized. In this study, we investigated the thermal degradation pathways of *ortho*-, *para*-, and *meta*-fluorofentanyl using a combination of ab initio molecular dynamics simulations and the enhanced sampling techniques of multiple walker metadynamics and umbrella sampling. We estimated the free energy profiles for each bond identified as a potential degradation site to elucidate the thermodynamic driving forces. Additionally, we predicted the forward attempt rate for each bond degradation reaction to assess its likelihood of breaking. Our findings indicate that, despite their structural similarities, fluorofentanyls differ in their degradation pathways.

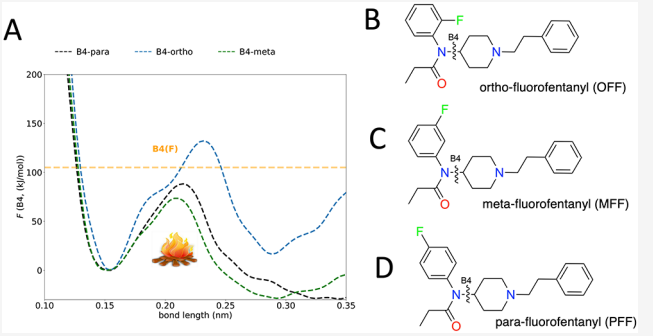

INTRODUCTION

Fentanyl and its analogs, particularly *ortho*-, *para*-, and *meta*-fluorofentanyl, have gained significant attention because of their increasing presence in the illicit drug market and their potential for abuse.[1] These analogs, which are chemically modified versions of fentanyl, are estimated to be highly potent than morphine.[1] Alongside fentanyl, a surge in the overuse of fluorofentanyls has been reported lately across the USA.[2−6] For example, the number of cases nationally involving fluorofentanyl overuse increased from 2 in 2016 to over 10,000 in 2021.[7] Of these different fluorofentanyls, studies show that fluorine atoms in the *ortho* position are more likely to cause overdose deaths than fluorine in the *para* and *meta* positions.[8,9]

The detection of fentanyl and its analogs are important for law enforcement officers, and a probe is needed to enable detection. While fentanyl in its undegraded state is easily detectable, its degradation makes it more challenging to identify the parent molecules from their degradation products.

Fentanyl degrades when exposed to heat.[10−12] While fentanyl and its analogs have been consumed by injecting, snorting, or ingesting, smoking is now the primary mode of use among drug overdose deaths in certain parts of the country.[1,13] Smoking exposes fentanyl to heat, which leads to degradation. The thermal degradation of fentanyl has been well studied.[10−12,14] In earlier work, we also studied the primary thermal degradation pathway of fentanyl analogs, specifically furanyl fentanyl and *ortho*-fluorofentanyl.[15] The degradation of *ortho*-, *para*-, and *meta*-fluorofentanyl yields despropionyl *ortho*-, *para*-, and *meta*-fentanyl. Those degradants are also reported to be among the opioids causing death.[5,16]

Structurally, the three fluorofentanyls (*ortho*-, *para*-, and *meta*-) share the same alkyl chain, piperidine ring, and amide group and the only difference is the fluorine atom, which occupies different positions on the phenyl ring (Figure 1). Despite close structural similarity, with the fluorine atom in the 2-, 3-, or 4- positions of the phenyl ring, these molecules may have different primary thermal degradation pathways. The possible fragments that could arise from the degradation of fluorofentanyls are shown in (Figure 2).

While the primary and secondary degradation reactions of fentanyl have been studied,[10−12,14,15,17] the degradation mechanism for fluorofentanyls, especially when the fluorine atoms are in different positions on the phenyl ring, has not been well studied. Higher overuse of fluorofentanyls compared to fentanyl is a recent phenomenon that has not generated

Received: April 21, 2025
Revised: December 9, 2025
Accepted: December 11, 2025
Published: December 16, 2025

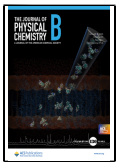

https://doi.org/10.1021/acs.jpcb.5c02722
J. Phys. Chem. B 2026, 130, 3−10

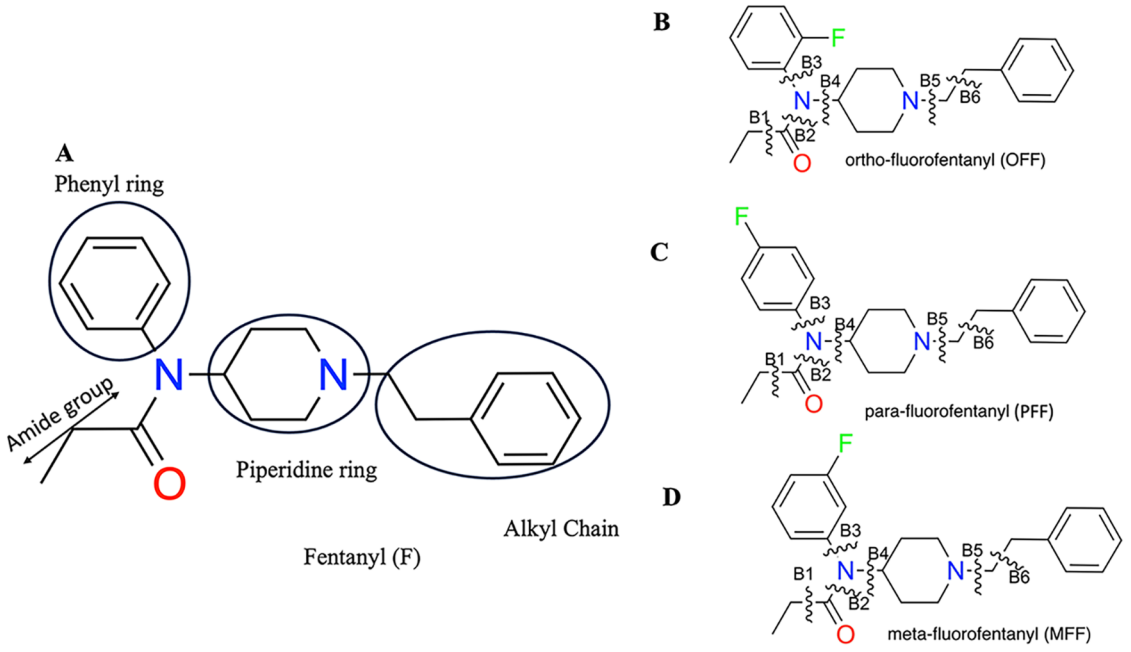

Figure 1. Chemical structures of fentanyl and fluorofentanyls along with the bonds of interest during thermal degradation: (A) fentanyl (F), with phenyl and piperidine rings and alkyl chain and amide group indicated; (B) *ortho*-fluorofentanyl (OFF); (C) *para*-fluorofentanyl (PFF); and (D) *meta*-fluorofentanyl (MFF).

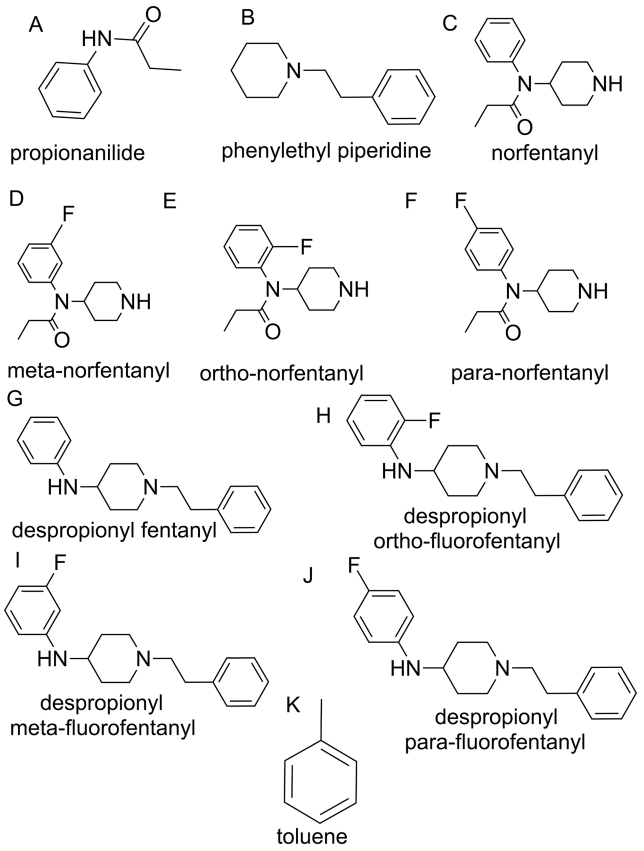

Figure 2. Possible fragments after degradation of fentanyl and fluorofentanyls. All fragments are taken from prior experimental studies.[10−12]

much attention. Here, we carry out a preliminary study of free energy for single bond breaking to facilitate comparisons between fluorofentanyls and fentanyl, along with the possible fragments formed after degradation, through extensive ab initio molecular dynamics (AIMD) simulations combined with the well-tempered multiple-walker metadynamics approach. We also calculate the forward attempt rate to cross the free energy barrier along the bond-breaking coordinates to gain insight into the bond-breaking mechanisms. The results may aid in making a device to detect fentanyl and its analogs in both degraded and undegraded forms.

METHODS

AIMD Simulations. AIMD simulations were performed using the Quickstep[18] module of the CP2K software package,[19] which facilitates density functional theory (DFT) calculations through the Gaussian and plane waves method (GPW). The local spin density (LSD) approximation was employed in all AIMD simulations to enable spin-unrestricted Kohn−Sham solutions. The PBE (Perdew Burke Ernzerhof) generalized gradient approximation[20] was used for the exchange-correlation functional in the electronic structure DFT calculations. Wave function optimization at each self-consistent field (SCF) step was carried out using the orbital transformation method[21] and direct inversion in the iterative subspace method, also known as Pulay mixing. A double-ζ basis set (DZVP-MOLOPT) was applied to all atoms, along with the Goedecker Teter Hutter (GTH) pseudopotentials.[22−25] Geometry optimization was performed using a conjugate gradient algorithm before running the MD simulation. A time step of 0.5 fs was selected for the dynamics. All simulations were conducted within a fixed rectangular cell with dimensions of 0.3 nm × 0.3 nm × 0.3 nm.

Our main goal is to analyze the bond breaking reactions of fluorofentanyls and compare them to the same reactions in the widely studied fentanyl molecule. Thus, a Nose-Hoover thermostat was employed in simulations to maintain a constant temperature of 1273 K. Experimentally, similarly high temperatures up to 1173 K were also used to study bond

https://doi.org/10.1021/acs.jpcb.5c02722
J. Phys. Chem. B 2026, 130, 3−10

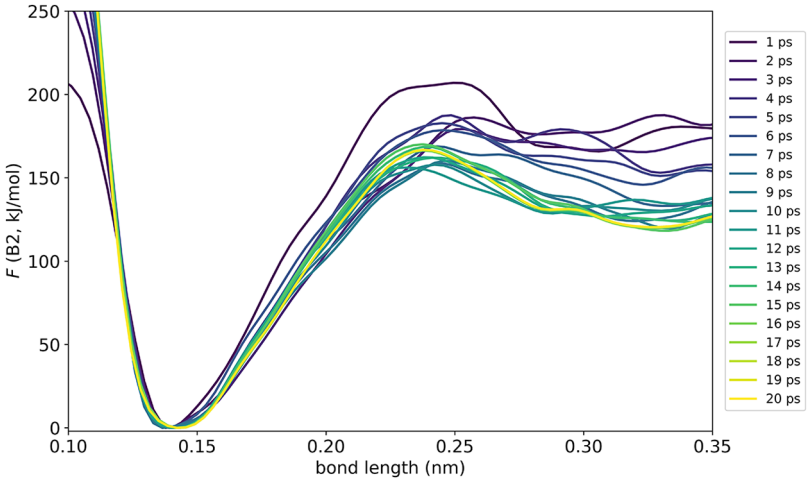

Figure 3. Energy convergence for the B2 bond of *meta*-fluorofentanyl. The free energy, $F(\mathrm{B2})$, was calculated at 1 ps intervals and plotted as a function of bond length. As illustrated, the free energy barrier converges over time.

breaking.[12] The use of a slightly elevated temperature in simulations, relative to experiment, may affect the energy barriers to bond breaking slightly, but the trends should remain largely unaffected. The additional benefit of a high simulation temperature is that the dynamics of the system are accelerated, enabling the free energy calculations to be carried out within the available simulation time scales of ps. The simulations were carried out in the gas phase to replicate the real world application where detection is performed in the absence of any medium.

Free Energy Calculations. Free energy calculations were performed with CP2K together with the PLUMED plugin.[26,27] The free energy computed here is a potential of mean force (PMF) and corresponds to the Helmholtz free energy as it is computed under constant temperature, but not constant pressure. The activation energy is determined by calculating the difference in free energy at the position of the maximum and the position of the minimum. Metadynamics-based methods have been used widely to determine reaction rate constants and have garnered considerable interest in the field of computational molecular science.[28,29] In addition, the well-tempered multiple walker metadynamics has been used for a wide range of systems, including transport proteins,[30] G protein-coupled receptors (GPCRs),[31] and the bond-breaking behavior of small molecules such as fentanyl.[14] In earlier studies, bond length was chosen as the reaction coordinate, which effectively captures the bond-breaking process along a single bond. While there are various ways of determining the reaction coordinate that contributes to molecular bond breaking, we chose the collective variable of bond length to make this study consistent with prior studies. The activation energies are connected to the kinetic rates of bond-breaking reactions via the Eyring equation from transition state theory.[32]

To calculate the activation free energy associated with bond breaking at specific bonds, we initially conducted steered molecular dynamics (MD) simulations, utilizing bond length (d) as the collective variable (CV) or reaction coordinate. A spring constant of 1,000,000 kJ/mol/nm^2 was applied for the time-dependent harmonic restraint potential, which progressively increases the bond length from its equilibrium position to an unbonded state, allowing us to select starting structures for determining the free energy along the bond coordinate. Thus, after completing the steered CV simulation, we selected 10 configurations at regular intervals along the bond CV and equilibrated each for 0.5 ps while maintaining a fixed harmonic potential on the bond lengths. These 10 configurations were then used to perform multiple-walker well-tempered metadynamics to determine the free energy along the specified reaction coordinates.[33,34] The activation energy, $\Delta F^{\dagger}$, is defined as the difference in free energy between the position of the maximum and the position of the minimum.

In the metadynamics runs, the simulations were biased with a time-dependent (t) potential (V) of the form

$$V(d, t) = \sum_{t'}^{t'<t} W \exp\left(- \frac{V(d(t'), t')}{k_B \Delta T} \right) \exp\left(- \frac{(d - d(t'))^2}{2\sigma^2} \right) \quad (1)$$

where W and σ are the height and width of the added Gaussian hills. ΔT is a fictitious maximum increase in temperature that ensures convergence by limiting the extent of the free energy exploration, and k_B is Boltzmann's constant.

At long time scales, the unbiased free energy, $F(d)$, can be recovered from

$$V(d, t \to \infty) = -\frac{\Delta T}{T + \Delta T} F(d) + C \quad (2)$$

where C is an immaterial constant. The value of ΔT is set by the 'bias factor' parameter, $b = \frac{T + \Delta T}{T}$, and the frequency of addition of Gaussian hills is determined by a fixed deposition rate, ω. The same values of σ = 0.01 nm, b = 15, W = 5.3 kJ/mol, and ω = 30 fs were used for all free energy calculations. The value of σ was chosen based on the standard deviation of the bond lengths observed during equilibrium simulations. Similarly, the value of ω was chosen to be greater than the typical period of oscillation of the bond lengths. The initial value of the hill height was chosen to be $\frac{k_B T}{2} = \frac{10.58 \text{ kJ / mol}}{2}$, where, k_B is the Boltzmann constant. The bias factor value of b = 15 was chosen so that a barrier on the order of 200 kJ/mol would be within reach of any given walker $\left(b < \frac{200 \text{ kJ / mol}}{10.58 \text{ kJ / mol}} = 19 \right)$. All walkers were run simultaneously in simulation time for approximately 20 ps each using well-

https://doi.org/10.1021/acs.jpcb.5c02722
J. Phys. Chem. B 2026, 130, 3−10

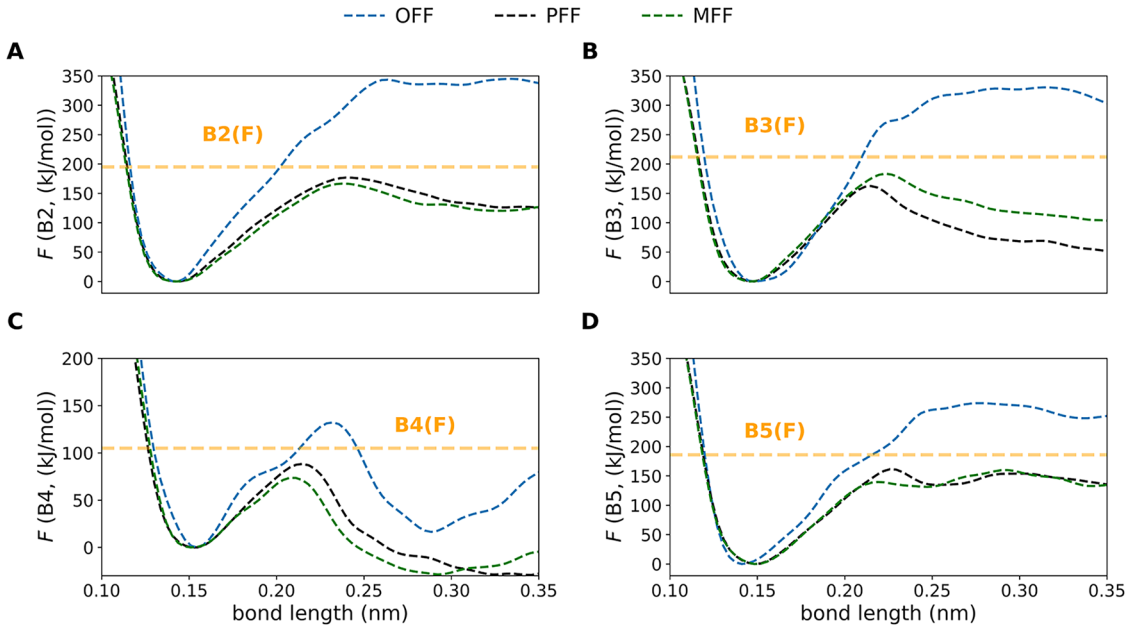

Figure 4. Free energy profiles of bond (between N and C atoms) breaking in fluorofentanyls estimated by enhanced sampling ab initio simulations at temperature 1273 K. Free energy is estimated using well-tempered metadynamics with the bond distance between atoms as the reaction coordinate. The horizontal orange dashed line is the bond breaking free energy of the same bonds in fentanyl, shown here for comparison with the fluorofentanyls. Panel (A) shows the bond breaking free energy landscapes of bond B2; (B) bond B3; (C) bond B4; and (D) bond B5.

tempered metadynamics. Therefore, the combined simulation time used to obtain each free energy surface is approximately 200 ps.

All the simulation settings are similar to our previously published work on fentanyl to enable direct comparison with the current results of fentanyl analogues.[14,15] While other approaches to computing free energy profiles are available, including umbrella sampling,[35] the metadynamics method has the advantage of not requiring prior knowledge of free energy barriers. Reweighting techniques, as discussed in earlier studies, provide an alternative approach to computing activation energies.[36] Convergence of the free energy profiles along the reaction coordinates was monitored by computing the difference between the maximum (F_{max}, at the transition barrier) and the minimum (F_{min}, at the length of the equilibrium bond) free energy values in 1 ps intervals per walker (Figures S1−S3). A sample free energy profile at the interval of 1 ps for bond B2 of *meta*-fluorofentanyl is shown in Figure 3. As described earlier, $F_{max} - F_{min}$ is the correct focus of convergence studies since activation free energy is the property of interest here.[37] The Python Matplotlib library was used to generate the plots.[38]

Temperature affects activation energy through the entropic component of free energy. Although running simulations at various temperatures would yield insights into how activation energies depend on temperature and on the balance between enthalpic and entropic contributions to activation energy, each simulation is computationally intensive and, therefore, beyond the scope of this study. Again, our focus here is on the trends in activation energies for bond breaking. The energy convergences of enhanced sampling are shown in Figures S1−S3 and the temperature convergence is shown in Figure S4. The exploration of configurational space by the walkers is shown in Figure S5 and evolution of Gaussian height over time is shown in Figure S6. Finally, the charge distribution of three fluorofentanyls is shown in Figure S7.

RESULTS AND DISCUSSION

Degradation Pathway of Fluorofentanyls. We followed a similar approach to our previous studies[14,15] in investigating the primary degradation pathways of fluorofentanyls (*ortho*-, *para*-, and *meta*-fluorofentanyl). We employed enhanced sampling techniques, including umbrella sampling followed by well-tempered multiple walkers metadynamics, to estimate the free energy associated with the breaking of specific bonds of interest, as shown in Figure 1. In this study, we categorized the bonds into two groups: (1) bonds formed by N and C atoms (B2, B3, B4, and B5), and (2) bonds formed by C−C atoms (B1 and B6). Previous studies identified the bond between the nitrogen atom on the piperidine ring (Figure 1) and its adjacent carbon atoms as a potential site for bond breaking.[10−12,14,39] The activation energy for bond breaking was calculated in the gas phase to simulate conditions relevant to fentanyl detection.

Initially, we utilized steered ab initio molecular dynamics simulations (AIMD) to stretch the bonds from their equilibrium bonded state (near 0.15 nm) to an unbonded state (near 0.60 nm) using steered harmonic potentials. This steered AIMD was followed by umbrella sampling and well-tempered metadynamics. We first estimated the bond breaking between the N and C atoms around the piperidine ring, noting that all three fluorofentanyls, as well as fentanyl, share the same piperidine ring.

Figure 4 illustrates the energetics of thermal degradation through breaking several bonds between N and C atoms. Starting with bond B2 (Figure 4A), we observe a similar bond-breaking pattern for *meta*- and *para*-fluoro fentanyls at approximately 200 kJ/mol, which aligns with the bond-breaking free energy of fentanyl (see orange dashed line). However, the bond-breaking free energy for *ortho*-fluoro fentanyl is higher, around 320 kJ/mol. This trend suggests that, when exposed to heat, the B2 bonds in *para*- and *meta*-fluorofentanyls are more likely to break compared to those in

https://doi.org/10.1021/acs.jpcb.5c02722
J. Phys. Chem. B 2026, 130, 3−10

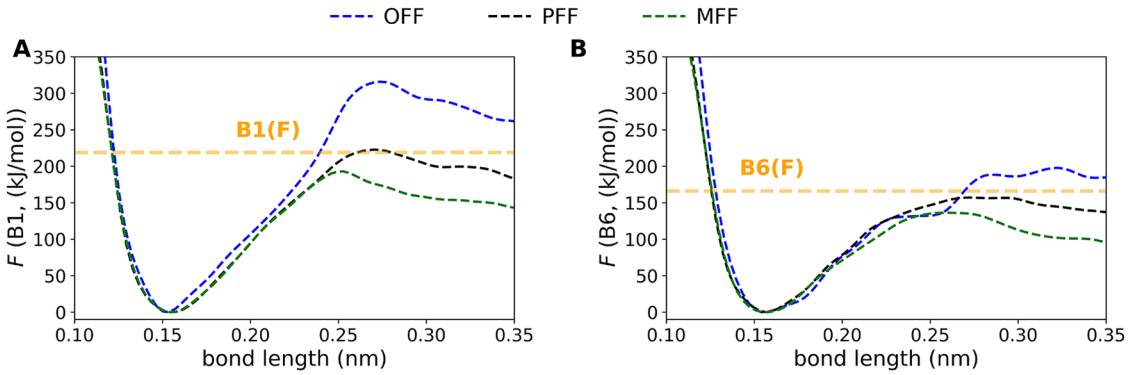

Figure 5. Free energy profiles of bond (between C and C atoms) breaking in fluorofentanyls estimated by enhanced sampling ab initio simulations at 1273 K. Free energy is estimated using well-tempered metadynamics with the bond distance between atoms as the reaction coordinate. The horizontal orange dashed line is the bond breaking free energy of the same bonds in fentanyl, shown here for comparison with the fluorofentanyls. Panel (A) shows the bond breaking free energy landscape for bond B1; (B) for bond B6.

ortho-fluorofentanyl. Breaking of bond B2 leads to the formation of *ortho*-, *para*-, *meta*-fluorofentanyls of despropionyl (Figure 2(G–J)), which also have potential for abuse. We find a similar trend in bond breaking for B3 (Figure 4B).

The bond-breaking pattern for bond B4 (Figure 4C) shows that all molecules have a lower bond-breaking free energy compared to the previously discussed B2 and B3 bonds. As mentioned earlier, breaking bond B4 results in the formation of propionanilide (PRP) and phenylethylpiperidine (PEP) in the case of fentanyl,[10−12] while the fluorofentanyls have not been studied per our knowledge. The fragment PEP is considered toxic due to the presence of the piperidine ring. The structures of PRP and PEP are included for completeness (Figure 2(A,B)).

The formation of PEP is highly probable in MFF, followed by PFF and OFF, as revealed by the free energy landscape. The bond-breaking free energy of B4 (105 kJ/mol) for fentanyl is lower than that of OFF (130 kJ/mol), but higher than that of PFF (88 kJ/mol) and MFF (74 kJ/mol). These results suggest that, when exposed to heat, the stability of bond B4 is greater in OFF compared to PFF and MFF, leading to a lower likelihood of PEP formation in OFF.

Another nitrogen atom from the piperidine ring that forms a bond with nearby carbon atoms (B5) was also examined in this study. The breaking of this bond results in norfentanyls for fentanyl (Figure 2C) while it yields *meta*-fluoro, *ortho*-fluoro and *para*-fluoro norfentanyl for MFF, OFF, and PFF, respectively (Figure 2(D–F)). All of these compounds are toxic, but to a lesser extent compared to fentanyl. The likelihood of forming *ortho*-fluoro norfentanyl is lower than that of *para*-fluoro norfentanyl and *meta*-fluoro norfentanyl, as indicated by the free energy barriers.

In addition to the bonds formed by N–C atoms, we also examined the likelihood of bond breaking between C–C atoms for B1 and B6 (Figure 5). The breaking of bond B6 results in the formation of toluene (Figure 2K), which is a toxic compound that can harm the liver and kidneys if ingested.[40] Following the trend observed for the N–C bonds, B1 and B6 exhibit a similar free energy profile. The likelihood of bond breaking for B1 and B6 is lower for OFF, followed by PFF and MFF, with fentanyl positioned between OFF and PFF.

Forward Attempt Rate to Cross Activation Energy Barrier for Bond Breaking. Challenges of characterizing the kinetics of bond breaking include a lack of feasibility for capturing rare events in simulations. Additionally, the computational cost may limit the ability to compute transitions between the reactant (bonded) and product (unbonded) states. To address these challenges, we estimated the forward attempt rates of bond breaking based on the free energy barrier at the highest value of the PMF along the reaction coordinate and the dissociation time (Table 1). We used an Arrhenius-

Table 1. Bond Breaking Dissociation time (t_D), Free Energy Barrier ($\Delta F^{\dagger}$), and Attempt Rate (k_f)[a]

bonds	t_D (ps)	$\Delta F^{\dagger}$ (kJ/mol)	k_f (s^{-1})	k_f/k_f (B4)
B1(F)	31.6	219 ± 2	3.1×10^{1}	2.2×10^{-5}
B1(OFF)	27.0	316 ± 2	4.0×10^{-3}	2.9×10^{-9}
B1(MFF)	20.0	193 ± 3	6.0×10^{1}	4.2×10^{-5}
B1(PFF)	16.0	222 ± 4	4.8×10^{1}	3.4×10^{-5}
B2(F)	39.4	195 ± 3	2.6×10^{2}	1.8×10^{-4}
B2(OFF)	4.0	336 ± 2	4.0×10^{-3}	2.9×10^{-9}
B2(MFF)	33.0	166 ± 4	5.0×10^{3}	3.6×10^{-3}
B2(PFF)	16.0	177 ± 5	3.4×10^{3}	2.4×10^{-3}
B3(F)	49.7	212 ± 4	4.1×10^{1}	2.9×10^{-5}
B3(OFF)	12.0	230 ± 6	3.1×10^{1}	2.2×10^{-5}
B3(MFF)	31.0	183 ± 2	1.0×10^{3}	7.1×10^{-3}
B3(PFF)	16.0	162 ± 4	1.4×10^{4}	1×10^{-2}
B4(F)	34.8	105 ± 2	1.4×10^{6}	$1.0 \times 10^{\circ}$
B4(OFF)	16.0	130 ± 1	2.8×10^{5}	2×10^{-1}
B4(MFF)	28.0	74 ± 2	3.2×10^{7}	2.3×10^{1}
B4(PFF)	14.0	88 ± 3	1.7×10^{7}	1.2×10^{1}
B5(F)	30.7	186 ± 1	7.1×10^{2}	5.1×10^{-4}
B5(OFF)	33.0	273 ± 1	1.9×10^{-1}	1.2×10^{-7}
B5(MFF)	27.0	160 ± 2	1.0×10^{4}	7.1×10^{-3}
B5(PFF)	14.0	161 ± 3	1.7×10^{4}	1.2×10^{-2}
B6(F)	34.1	166 ± 1	4.5×10^{3}	3.2×10^{-3}
B6(OFF)	7.0	197 ± 7	1.2×10^{3}	8.5×10^{-4}
B6(MFF)	27.0	136 ± 2	9.7×10^{4}	6.9×10^{-2}
B6(PFF)	12.0	157 ± 4	3.0×10^{4}	2.1×10^{-2}

[a]All the forward rates (k_f) are computed relative to bond B4 of fentanyl.

Bell model to estimate the forward attempt rate, which represents the likelihood of reactants overcoming the free energy barrier.[41,42] All attempt rates for OFF, PFF and MFF are computed relative to the rate for B4 of fentanyl. The attempt rate can be estimated using

https://doi.org/10.1021/acs.jpcb.5c02722
J. Phys. Chem. B 2026, 130, 3−10

$$k_f = \frac{1}{t_D} \exp\left(\frac{-\Delta F^{\dagger}}{k_B T}\right) \quad (3)$$

where t_D is the diffusive relaxation time, $\Delta F^{\dagger}$ difference in free energy between the values at the peak (transition state) and the equilibrium bond length along the reaction pathway, k_B is the Boltzmann constant and T is the temperature. The diffusive relaxation time is the inverse of the bond vibrational frequency and is computed by quantifying the temporal variations in bond distances during the equilibrium (unbiased) simulations. We used Fourier analysis to extract the frequencies associated with these bond fluctuations.[43,44]

The forward attempt rate, k_f, depends on the spontaneous dissociation rate and on the difference in the free energy between the two states (reactant and transition states). Since k_f is exponentially related to the difference in free energy, as shown in eq 3, even a small change in free energy changes k_f significantly. We calculated the ratio of the forward attempt rate of all bonds to the forward attempt rate of B4 ($k_f/k_f(B4)$) to estimate the likelihood of bond breaking. The B4 bond of MFF and PFF show 23 and 12 times higher propensity to degradation as compared to the B4 bond of fentanyl. The analysis shows all bonds of MFF and PFF studied here are prone to degrade easily, followed by bonds in fentanyl and OFF.

In our study, we utilized DFT without incorporating dispersion corrections. Previous research has indicated that dispersion-corrected DFT does not demonstrate improved performance in ionic systems[45] although it has shown enhanced accuracy in other types of systems.[46−50] While our results may have limitations due to the absence of dispersion corrections, the calculation of activation energies ($\Delta F^{\dagger}$), determined as the difference between two extrema, effectively mitigates potential errors.

CONCLUSION

We carried out a comprehensive ab initio molecular dynamics study combined with enhanced sampling techniques to investigate the bond-breaking free energies of fluorofentanyls. Through extensive ab initio molecular dynamics simulations, totaling over 750 ps, our results demonstrate that even minor structural changes can lead to significant differences in bond-breaking pathways.

Utilizing well-tempered multiple walkers metadynamics, we computed the activation free energy associated with bond breaking. Our findings indicate the *ortho*-fluorofentanyl (OFF) molecule exhibits the strongest bonds among the molecules studied. The higher activation free energy associated with OFF suggests a lower probability of bond breaking. Specifically, when comparing the activation free energy of the bond most likely to break first across all cases (B4), OFF has an activation energy of 130 kJ/mol, while *F* has 105 kJ/mol, followed by MFF and PFF with activation energies of 74 and 88 kJ/mol, respectively. In addition to activation free energy, we calculated the forward attempt rate kinetics to assess the likelihood of bonds escaping their equilibrium state. Consistent with the free energy profiles, our results show that OFF has the lowest forward attempt rate, whereas MFF exhibits the highest rate in most cases, except for bond B3.

The primary objective of this study was to contribute to the development of a device for detecting fentanyl and its analogs in both degraded and undegraded forms. Our findings estimated the probability of compound formation following degradation, which can be helpful in the design of such a detection device. Additionally, in future work, these results may be extended to investigate the degradation pathways in the presence of various media and substrates.

ASSOCIATED CONTENT

Supporting Information

The Supporting Information is available free of charge at https://pubs.acs.org/doi/10.1021/acs.jpcb.5c02722.

Additional figures showing possible fragments of the fluorofentanyls and the partial charges along with the convergence of AIMD and enhanced sampling simulations (PDF)

AUTHOR INFORMATION

Corresponding Authors

Bharat Poudel − *Environmental Systems Biology, Sandia National Laboratories, Albuquerque, New Mexico 87123, United States*; orcid.org/0009-0001-8684-1171; Email: bpoudel@sandia.gov

Susan B. Rempe − *Retired, Sandia National Laboratories, Albuquerque, New Mexico 87123, United States*; Email: slbrabq@gmail.com

Authors

Joshua J. Whiting − *Biological and Chemical Sensors, Sandia National Laboratories, Albuquerque, New Mexico 87123, United States*

Juan M. Vanegas − *Department of Biochemistry and Biophysics, Oregon State University, Corvallis, Oregon 97333, United States*

Complete contact information is available at: https://pubs.acs.org/10.1021/acs.jpcb.5c02722

Notes

Distribution Statement A. Approved for Public Release. Distribution Unlimited.

The authors declare no competing financial interest.

ACKNOWLEDGMENTS

The authors appreciate funding from the Department of Defense. This work was performed, in part, at the Center for Integrated Nanotechnologies, an Office of Science User Facility operated for the U.S. Department of Energy (DOE) Office of Science. Computations were performed, in part, on the Vermont Advanced Computing Core supported in part by NSF Award No. OAC-1827314. Sandia National Laboratories is a multimission laboratory managed and operated by National Technology & Engineering Solutions of Sandia, LLC (NTESS), a wholly owned subsidiary of Honeywell International Inc., for the U.S. Department of Energys National Nuclear Security Administration (DOE/NNSA) under the DE-NA0003525 contract. This written work is authored by an employee of NTESS. The employee, not NTESS, owns the right, title and interest in and to the written work and is responsible for its contents. Any subjective views or opinions that might be expressed in the written work do not necessarily represent the views of the US Government. The publisher acknowledges that the U.S. Government retains a nonexclusive, paid-up, irrevocable, worldwide license to publish or reproduce the published form of this written work or allow others to do

so, for U.S. Government purposes. The DOE will provide public access to results of federally sponsored research in accordance with the DOE Public Access Plan.

REFERENCES

(1) O'Donnell, J. K.; Halpin, J.; Mattson, C. L.; Goldberger, B. A.; Gladden, R. M. Deaths Involving Fentanyl, Fentanyl Analogs, and U-47700 — 10 States, July–December 2016. *Morb. Mortal. Wkly. Rep. (MMWR)* **2017**, *66*, 1197–1202, DOI: 10.15585/mmwr.mm6643e1.

(2) Schueler, H. E. Emerging Synthetic Fentanyl Analogs. *Acad. Forensic Pathol.* **2017**, *7*, 36–40.

(3) Bitting, J.; O'Donnell, J.; Mattson, C. L. Notes from the Field: Overdose Deaths Involving Para-fluorofentanyl - United States, July 2020–June 2021. *Morb. Mortal. Wkly. Rep. (MMWR)* **2021**, *39*, 1239–1240.

(4) Helland, A.; Brede, W. R.; Michelsen, L. S.; Gundersen, P. O. M.; Aarset, H.; Skjølås, J. E.; Slørdal, L. Two Hospitalizations and One Death After Exposure to Ortho-Fluorofentanyl. *J. Anal. Toxicol.* **2017**, *41*, 708–709.

(5) City and County of San Francisco: Report on Novel Synthetic Opioid and Xylazine Re-Analysis of 2022 Accidental Overdoses. https://tinyurl.com/mvu3rkpu. (Accessed: 2023).

(6) Schedules of Controlled Substances: Temporary Placement of ortho-Fluorofentanyl, Tetrahydrofuranyl Fentanyl, and Methoxyacetyl Fentanyl Into Schedule I. https://tinyurl.com/3aets3ps. (Accessed: 2017).

(7) National Forensic Laboratory Information System: NFLIS-DRUG 2021 Annual Report. https://tinyurl.com/44uncn54. (Accessed: 2021).

(8) Erkok, S. D.; Guray, T.; McCord, B. Detection of para, ortho, meta-fluorofentanyl by surface-enhanced Raman spectroscopy. *Forensic Chem.* **2024**, *38*, No. 100559.

(9) Kanamori, T.; Okada, Y.; Segawa, H.; Yamamuro, T.; Kuwayama, K.; Tsujikawa, K.; Iwata, Y. T. Evaluation of Agonistic Activity of Fluorinated and Nonfluorinated Fentanyl Analogs on μ-Opioid Receptor Using a Cell-Based Assay System. *Biol. Pharm. Bull.* **2021**, *44*, 159–161.

(10) Nishikawa, R. K.; Bell, S. C.; Kraner, J. C.; Callery, P. S. Potential biomarkers of smoked fentanyl utilizing pyrolysis gas chromatography-mass spectrometry. *J. Anal. Toxicol.* **2009**, *33*, 418–422.

(11) Garg, A.; Solas, D. W.; Takahashi, L. H.; Cassella, J. V. Forced degradation of fentanyl: Identification and analysis of impurities and degradants. *J. Pharm. Biomed. Anal.* **2010**, *53*, 325–334.

(12) Manral, L.; Gupta, P. K.; Suryanarayana, M. V. S.; Ganesan, K.; Malhotra, R. C. Thermal Behaviour of fentanyl and its analogues during flash pyrolysis. *J. Therm. Anal. Calorim.* **2009**, *96*, 531–534.

(13) Oregon Health Authority. Fentanyl 2024 https://tinyurl.com/5h4jf4sn. (Accessed: 2024).

(14) Poudel, B.; Monteith, L.; Haley; Sammon, J. P.; Whiting, J. J.; Moorman, M. W.; Vanegas, J. M.; Rempe, S. B. Energetics of high temperature degradation of fentanyl into primary and secondary products. *Phys. Chem. Chem. Phys.* **2023**, *25*, 30880–30886.

(15) Poudel, B.; Whiting, J. J.; Vanegas, M. J.; Rempe, S. S. Thermal degradation energetics of fentanyl and its analogues: furanyl fentanyl and ortho-fluoro fentanyl. *Phys. Chem. Chem. Phys.* **2025**, *27*, 9631–9636.

(16) Daniulaityte, R.; Juhascik, M. P.; Strayer, K. E.; Sizemore, I. E.; Harshbarger, K. E.; Antonides, H. M.; Carlson, R. R. Overdose Deaths Related to Fentanyl and Its Analogs - Ohio 2017 https://www.cdc.gov/mmwr/volumes/66/wr/mm6634a3.htm.

(17) Rabinowitz, J. D.; Wensley, M.; Lloyd, P.; Myers, D.; Shen, W.; Lu, A.; Hodges, C.; Hale, R.; Mufson, D.; Zaffaroni, A. Fast onset medications through thermally generated aerosols. *J. Pharmacol. Exp. Ther.* **2004**, *309*, 769–775.

(18) VandeVondele, J.; Krack, M.; Mohamed, F.; Parrinello, M.; Chassaing, T.; Hutter, J. Quickstep: Fast and accurate density functional calculations using a mixed Gaussian and plane waves approach. *Comput. Phys. Commun.* **2005**, *167*, 103–128.

(19) Kühne, T. D.; Iannuzzi, M.; Del Ben, M.; Rybkin, V. V.; Seewald, P.; Stein, F.; Laino, T.; Khaliullin, R. Z.; Schütt, O.; Schiffmann, F.; et al. CP2K: An electronic structure and molecular dynamics software package - Quickstep: Efficient and accurate electronic structure calculations. *J. Chem. Phys.* **2020**, *152*, No. 194103.

(20) Perdew, J. P.; Burke, K.; Ernzerhof, M. Generalized Gradient Approximation Made Simple. *Phys. Rev. Lett.* **1996**, *77*, No. 3865.

(21) VandeVondele, J.; Hutter, J. An efficient orbital transformation method for electronic structure calculations. *J. Chem. Phys.* **2003**, *118*, 4365–4369.

(22) VandeVondele, J.; Hutter, J. Gaussian basis sets for accurate calculations on molecular systems in gas and condensed phases. *J. Chem. Phys.* **2007**, *127*, No. 114105.

(23) Goedecker, S.; Teter, M.; Hutter, J. Separable dual-space Gaussian pseudopotentials. *Phys. Rev. B* **1996**, *54*, No. 1703.

(24) Hartwigsen, C.; Goedecker, S.; Hutter, J. Relativistic separable dual-space Gaussian pseudopotentials from H to Rn. *Phys. Rev. B* **1998**, *58*, No. 3641.

(25) Krack, M. Pseudopotentials for H to Kr optimized for gradient-corrected exchange-correlation functionals. *Theor. Chem. Acc.* **2005**, *114*, 145–152.

(26) Bonomi, M.; Branduardi, D.; Bussi, G.; Camilloni, C.; Provasi, D.; Raiteri, P.; Donadio, D.; Marinelli, F.; Pietrucci, F.; Broglia, R. A.; Parrinello, M. PLUMED: A portable plugin for free-energy calculations with molecular dynamics. *Comput. Phys. Commun.* **2009**, *180*, 1961–1972.

(27) Tribello, G. A.; Bonomi, M.; Branduardi, D.; Camilloni, C.; Bussi, G. PLUMED 2: New feathers for an old bird. *Comput. Phys. Commun.* **2014**, *185*, 604–613.

(28) Ray, D.; Parrinello, M. Kinetics from Metadynamics: Principles, Applications, and Outlook. *J. Chem. Theory Comput.* **2023**, *19*, 5649–5670.

(29) Kang, P.; Trizio, E.; Parrinello, M. Computing the committor with the committor to study the transition state ensemble. *Nat. Comput. Sci.* **2024**, *4*, 451–460.

(30) Prignano, L. A.; Stevens, M. J.; Vanegas, J. M.; Rempe, S. B.; Dempski, R. E. Metadynamics simulations reveal mechanisms of Na^+ and Ca^{2+} transport in two open states of the channelrhodopsin chimera, C1C2. *PLoS One* **2024**, *19*, No. e0309553.

(31) Poudel, B.; Rajitha, R. T.; Vanegas, J. M. Membrane mediated mechanical stimuli produces distinct active-like states in the AT1 receptor. *Nat. Commun.* **2023**, *14*, No. 4690.

(32) Rooney, J. J. Eyring transition-state theory and kinetics in catalysis. *J. Mol. Catal. A: Chem.* **1995**, *96*, 1–3.

(33) Raiteri, P.; Laio, A.; Gervasio, F. L.; Micheletti, C.; Parrinello, M. Efficient Reconstruction of Complex Free Energy Landscapes by Multiple Walkers Metadynamics. *J. Phys. Chem. B* **2006**, *110*, 3533–3539.

(34) Barducci, A.; Bussi, G.; Parrinello, M. Well-Tempered Metadynamics: A Smoothly Converging and Tunable Free-Energy Method. *Phys. Rev. Lett.* **2008**, *100*, No. 020603.

(35) Priest, C.; VanGordon, M. R.; Rempe, C. S.; Chaudhari, M. I.; Stevens, M. J.; Rick, S.; Rempe, S. B. *Channel Rhodopsin: Methods and Protocols*; Dempski, R. E., Ed.; Springer US: New York, NY, 2021; pp 17–28.

(36) Bal, K. M.; Fukuhara, S.; Shibuta, Y.; Neyts, E. C. Free energy barriers from biased molecular dynamics simulations. *J. Chem. Phys.* **2020**, *153*, No. 114118.

(37) Rempe, S. B.; Mattsson, T. R.; Leung, K. On "the complete basis set limit" and plane-wave methods in first-principles simulations of water. *Phys. Chem. Chem. Phys.* **2008**, *10*, 4685–4687.

(38) Hunter, J. D. Matplotlib: A 2D graphics environment. *Comput. Sci. Eng.* **2007**, *9*, 90–95.

(39) Bazley, M.; Logan, M.; Baxter, C.; Robertson, A. A. B.; Blanchfield, J. T. Decontamination of Fentanyl and Fentanyl

Analogues in Field and Laboratory Settings: A Review of Fentanyl Degradation. *Aust. J. Chem.* **2020**, 868−879.
(40) Holmes, M. D.; Murrat, B. P. *Toulene Toxicity*; StatPearls Publishing LLC, 2024.
(41) Vanegas, J. M.; Arroyo, M. Force Transduction and Lipid Binding in MscL: A Continuum-Molecular Approach. *PLoS One* **2014**, *9* (12), No. e113947.
(42) Evans, E. Probing the relation between force-lifetime-and chemistry in single molecular bonds. *Annu. Rev. Biophys. Biomol. Struct.* **2001**, *30*, 105−128.
(43) Rempe, S. B.; Jónsson, H. A computational exercise illustrating molecular vibrations and normal modes. *Chem. Educ.* **1998**, *3*, 1−17.
(44) Muralidharan, A.; Chaudhari, M. I.; Pratt, L. R.; Rempe, S. B. Molecular Dynamics of Lithium Ion Transport in a Model Solid Electrolyte Interphase. *Sci. Rep.* **2014**, *8*, No. 10736.
(45) Soniat, M.; Rogers, D. M.; Rempe, S. B. Dispersion- and Exchange-Corrected Density Functional Theory for Sodium Ion Hydration. *J. Chem. Theory Comput.* **2015**, *11*, 2958−2967.
(46) Grimme, S.; Ehrlich, S.; Goerigk, L. Effect of the damping function in dispersion corrected density functional theory. *J. Comput. Chem.* **2011**, *32*, 1456−1465.
(47) Grimme, S.; Steinmetz, M. Effects of London dispersion correction in density functional theory on the structures of organic molecules in the gas phase†. *Phys. Chem. Chem. Phys.* **2013**, *15*, 16031−16042.
(48) Goerigk, L. H. How Do DFT-DCP, DFT-NL, and DFT-D3 Compare for the Description of London-Dispersion Effects in Conformers and General Thermochemistry? *J. Chem. Theory Comput.* **2014**, *10*, 968−980.
(49) Chai, J. D.; Head-Gordon, M. Long-Range Corrected Hybrid Density Functionals with Damped Atom-Atom Dispersion Corrections. *Phys. Chem. Chem. Phys.* **2008**, *10*, 6615−6620.
(50) Fogueri, U. R.; Kozuch, S.; Karton, A.; Martin, J. M. L. The Melatonin Conformer Space: Benchmark and Assessment of Wave Function and DFT Methods for a Paradigmatic Biological and Pharmacological Molecule. *J. Phys. Chem. A* **2013**, *117*, 2269−2277.

https://doi.org/10.1021/acs.jpcb.5c02722
J. Phys. Chem. B 2026, 130, 3−10